A salt cavern abandonment test

P. Bérest[a], J. Bergues[a], B. Brouard[a],*, J.G. Durup[b], B. Guerber[b]

[a] *Laboratoire de Mécanique des Solides, Ecole Polytechnique, 91128 Palaiseau, France*
[b] *Gaz de France, DR/DRS/SIM, 361, av. du Président Wilson - BP 33, 93211 La Plaine Saint Denis, France*

Abstract

Thousands of caverns have been leached out from deep salt formations. They are used for saturated brine production and/or hydrocarbons storage. They will be abandoned some day: the access well will be plugged with cement, isolating a large bubble of saturated brine. The later evolution of such a bubble raises serious concerns for environmental protection; salt creep and brine thermal expansion can lead to brine pressure build-up and rock-mass fracture, then brine seepage can lead to pollution of overlying water-bearing strata. Taking into account salt formation permeability leads to less pessimistic scenarios. An 18-month test has been performed on a deep brine-filled cavern. The objective was to measure the brine equilibrium pressure reached when the cavern is closed. Such an equilibrium is reached when salt mass creep, which leads to cavern shrinkage, balances brine permeation through the cavern wall. This objective was met by imposing different pressure levels and observing whether the pressure increased (or decreased) with respect to time. Data misinterpretation (i.e., a well leak instead of a cavern-proper leak) was precluded by a special monitoring system. The observed equilibrium pressure was significantly smaller than geostatic pressure, alleviating any fracture risk for a sealed and abandoned cavern in this salt formation. © 2001 Elsevier Science Ltd. All rights reserved.

1. Introduction

In the past several years, there has been concern about the thermohydromechanical behavior of deep underground salt caverns after they have been sealed and abandoned. By "deep", we mean caverns whose depths range between 500 and 2000 m. These caverns have been leached out from salt formations: a (typically) 1-km deep well is cased and cemented to the rock formation; its shoe is anchored to the top of the salt formation. A smaller central tube allows soft water injection at the bottom of the cavern: after leaching out of soluble rock-salt, brine is removed from the cavern through the annular space between cemented casing and central injection tube. After 1 year or more, a 10,000–1,000,000 m³ cavern has been created. Fig. 4 displays a typical cavern cross-section. In many cases the cavern is later used for hydrocarbons storage (crude oil, LPG or natural gas). These caverns will be abandoned some day. Interest in the very long-term behavior of such

abandoned caverns has increased due to increasing concern for environmental protection, on one hand, and to several new projects in which caverns are used for disposal of non-hazardous, industrial or even low-level nuclear wastes, on the other. The *Solution Mining Research Institute* which represents companies, consultants and research centers involved in the solution mining industry has set this problem at the center of its research program and has supported the test described in this paper.

Most experts agree on the following general scenario. In most cases, prior to abandonment, the cavern will be filled with brine. Its initial pressure when the cavern is closed will result from the weight of a brine column filling the well from the surface to the cavern. Hereafter, this pressure will be called the *halmostatic pressure*; it is equal to P_h (MPa) $= 0.012H$ (m) [or P_h (psi) $= 0.52H$ (feet)], where H is the average cavern depth ($H = 950$ m for the Ez53 cavern to be discussed later). Then a special steel plug will be set at casing seat and cement will be poured in the well, isolating a large "bubble" of fluid whose future evolution is the main concern of the present paper. After the cavern is closed

---

*Corresponding author. Tel.: + 33-01-69-334128; fax: + 33-01-69-333026.

and abandoned, cavern brine pressure will build up. Results of the several so-called "shut-in pressure tests" clearly support this view [1–6].

The final value of cavern brine pressure is of utmost importance from the environmental protection point of view. In salt formation, the natural state of stress resulting from overburden weight is generally assumed to be isotropic; this geostatic pressure is P_∞ (MPa) $= 0.022H$ (m) at cavern depth. Several authors think that in many cases brine pressure will after some time reach a figure larger than the geostatic pressure, then leading to hydrofracturing; brine will flow upward through fractures, to shallow water-bearing strata, leading to water pollution, cavern collapse and subsidence. Consequences will be more severe when the cavern contains wastes [7]. To which point this pessimistic scenario can be alleviated by taking into account salt permeability will be discussed later.

Physical mechanisms governing pressure build up must be identified (Fig. 1). The role of cavern creep has been clearly identified, for instance by Langer et al. [8], Wallner [9], Cauberg et al. [10], Van Sambeek [3], Bérest [11], Rolfs et al. [12], Wallner and Paar [13]: salt mass creep leads to cavern shrinkage; cavern brine is offered smaller room and its pressure builds up in a sealed cavern. The process is slower when cavern pressure is high, and ultimately stops when cavern pressure is equal to geostatic. Bérest et al. [1] outlined the role played by brine thermal expansion: temperature distribution after cavern creation is out of equilibrium, brine is significantly cooler than salt mass; heat transfer from the salt mass leads to brine warming, thermal expansion and pressure build up. This idea has also been discussed by Hugout [14], Ehgartner and Linn [15], Bérest et al. [16]. Bérest [11] suggested that brine transfer to the salt formation through permeation–like phenomena is also to be taken into account. Cosenza and Ghoreychi [17] proposed a set of equations governing pressure evolution in a sealed and abandoned cavern. Further contributions by Cosenza and Ghoreychi [18],
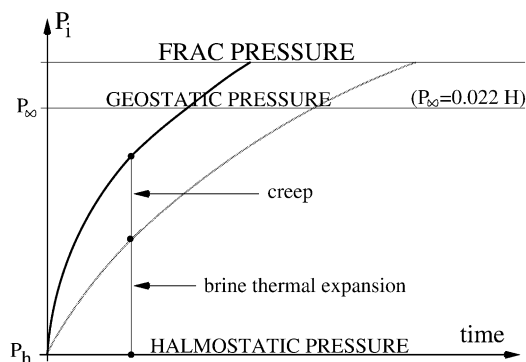
Bérest et al. [16], Pfeifle et al. [19] analyzed the role of this factor: even if exceedingly small in terms of yearly fluid flow, brine transfer can lead to significant pressure release. The present paper describes an in-situ test which is probably the first attempt to support by field evidence the notion of pressure relief by salt (micro) permeability.

2. Mechanisms affecting the brine pressure evolution

2.1. Salt creep

The mechanical behavior of salt exhibits a fascinating complexity, and several aspects of it are still open to discussion; see, for instance, the proceedings of the four "Conferences on the Mechanical Behavior of Salt" [20–23]. However, experts do agree on several features of importance to the problem under discussion.

(a) Salt behaviour is elastic-ductile, when short-term compression tests are considered, and elastic-fragile when tensile tests are considered; but in the long term, salt behaves as a fluid in the sense that it flows even under very small deviatoric stresses.

(b) Creep rate is a highly non-linear function of applied deviatoric stress and test temperature.

Furthermore, experts generally distinguish between (Fig. 2).

(i) steady-state (or secondary) creep, which is reached after some time (several weeks) when a constant mechanical loading is applied to a rock sample; steady state is characterized by a constant creep rate, which is a function of the (constant) temperature and stress applied during a test; and

(ii) transient (or primary) creep, which is triggered when the stress applied to a sample is suddenly changed. Transient creep is characterized by high initial rates (following a load increase) that slowly reduce to reach steady-state creep or by slow, sometimes reverse, initial rates (following a load decrease) that slowly increase to reach steady-state creep (see [24]).

A similar distinction between steady-state and transient behavior can be made in a salt cavern, when, instead of sample axial strain rate ($\dot{\varepsilon}$), we consider the volumetric strain rate of the cavern ($\dot{V}/V$) and, instead of the uniaxial stress applied on the sample, we consider the difference ($P_\infty - P_i$) between the natural geostatic pressure (P_∞) at cavern depth and the internal brine pressure in the cavern (P_i). However, the analogy must be slightly corrected. On one hand, transient mechanical effects in a brine-filled cavern actually combine with the additional dissolution (or crystallization) that is triggered by any pressure increase (or decrease), leading to more pronounced transient effects; on the other hand, mechanical transient effects in a cavern can last much longer than in a rock sample; stress distribution is not
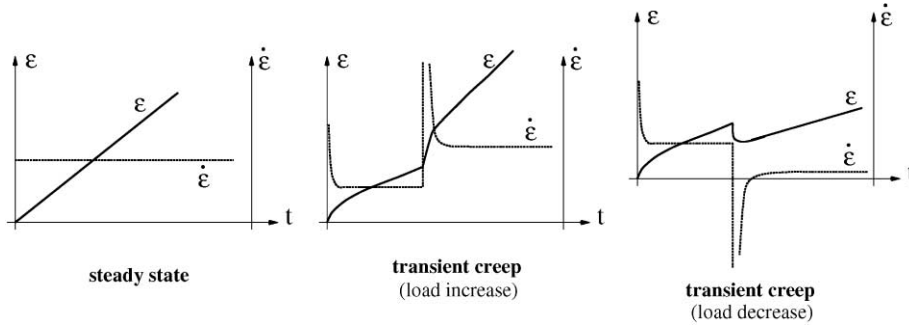

Fig. 1. Pressure build-up in a closed cavern leads to fracturing. Pressure build up is due to (i) brine thermal expansion (ii) creep.

Fig. 2. Steady-state creep, transient creep during a uniaxial creep test; ε is the absolute (positive) axial strain.
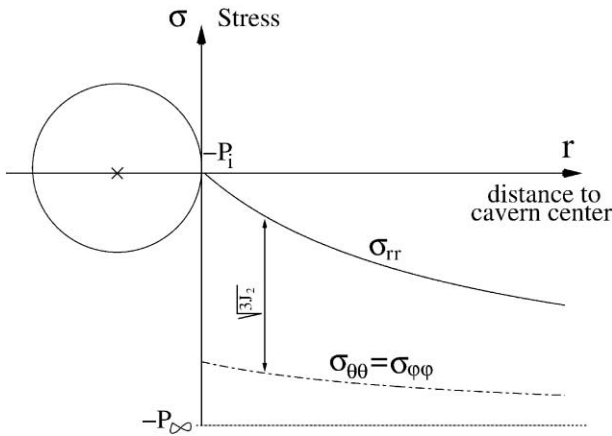

Fig. 3. Stress distribution in a hollow sphere; sphere external radius is supposed to be much larger than cavity radius. In this case $\sqrt{3J_2} = \sigma_{rr} - \sigma_{\theta\theta}$ is the difference between the radial main stress (σ_{rr}) and the tangential main stress ($\sigma_{\theta\theta} = \sigma_{\varphi\varphi}$). At large distance from the cavern wall (not represented in the figure), the tangential stress is smaller than the geostatic stress ($-P_\infty$).

uniform in the vicinity of a cavity, in contrast with the situation which prevails during a uniaxial test, and stress change due to brine pressure change must propagate throughout the rock mass before steady-state behavior is reached; in other words, cavern transient behavior results from salt transient rheological behavior combined with a factor of geometrical origin.

Returning to the uniaxial behavior of a rock sample, the steady-state creep behavior is described by the following expression, sometimes called the Norton–Hoff (or power) law:

$$\dot{\varepsilon} = A \exp\left(-\mathcal{Q}/\mathcal{R}T\right)\sigma^n,$$

where A, n and $-\mathcal{Q}/\mathcal{R}$ are three parameters, σ is the uniaxial applied stress and T is the (absolute) test temperature. The exponent n ranges from 3 to 6, and $\mathcal{Q}/\mathcal{R}$ ranges from 4000 to 10,000 K. A compilation of data published in the literature can be found in Brouard and Bérest [25].

This uniaxial expression can be generalized in a 3D formulation:

$$\dot{\underline{\varepsilon}} = A \exp\left(-\mathcal{Q}/\mathcal{R}T\right)\frac{1}{n+1}\frac{\partial\left(\sqrt{3J_2}\right)^{n+1}}{\partial \underline{\sigma}},$$

where $J_2 = \frac{1}{2}s_{ij}s_{ji}$, $s_{ij} = \sigma_{ij} - \frac{1}{3}(\sigma_{ii})\delta_{ij}$.

Using this formulation, a closed-form solution can be obtained for the idealized case of a perfectly spherical (or cylindrical) cavern that, over a long period of time, is subjected to an internal pressure (P_i) smaller than the natural geostatic pressure (P_∞) at cavern depth. Stress distribution is displayed in Fig. 3. Note that at large distance from the cavern wall (not shown in the figure) the tangential stress is smaller than the geostatic stress, $\sigma_{\theta\theta} + P_\infty < 0$, achieving forces balance along any cross-section.

For a spherical cavern, the steady-state relation between volume rate change, temperature and pressure is as follows:

$$\frac{\dot{V}}{V} = -\frac{3}{2}\left[\frac{3}{2n}(P_\infty - P_i)\right]^n A \exp\left(-\frac{\mathcal{Q}}{\mathcal{R}T}\right). \quad (1)$$

A similar formula for a cylindrical cavern has been given by Van Sambeek [3]:

$$\frac{\dot{V}}{V} = -\sqrt{3}\left[\frac{\sqrt{3}}{n}(P_\infty - P_i)\right]^n A \exp\left(-\frac{\mathcal{Q}}{\mathcal{R}T}\right). \quad (2)$$

An immediate consequence of the first above-mentioned feature (a), which is captured by formula (1) and (2), is that, as long as the cavern fluid pressure is smaller than the geostatic pressure (which it is when the cavern is abandoned and sealed in halmostatic conditions, $P_i = P_h$), the cavern shrinks, leading to cavern pressure build-up in a closed cavern.

A typical value of the initial shrinkage rate for a 1000-m deep cavern is $\dot{V}/V = -3 \times 10^{-4}$ yr^{-1}, although there are large variations according to site-specific salt properties and cavern shape (see Brouard and Bérest [25]). Such a shrinkage rate in a closed cavern will lead to a pressure build-up rate of $\dot{P}_i = -\dot{V}/(\beta V)$, where β is the cavern compressibility factor. In a standard

cavern, $\beta \approx 4 \times 10^{-4}\,\text{MPa}^{-1}$ or $3 \times 10^{-6}\,\text{psi}^{-1}$ and $\dot{P}_i \approx 0.75\,\text{MPa/yr}$ (see [26]). However, significantly larger values of the cavern compressibility factor (and, consequently, smaller values of the initial pressure build-up rate $\dot{P}_i$) can be found either because cavern shape is irregular (flat, or "penny-shaped", for instance), or because the cavern contains gas pockets (see [27]). It must be noted that pressure build-up progressively leads to smaller creep rates, because the difference $(P_\infty - P_i)$ between geostatic pressure at cavern depth and cavern fluid pressure reduces with time. Equilibrium — i.e., exact balance between brine average pressure and geostatic average pressure at cavern depth — will not be reached for several centuries, as pointed out by Wallner and Paar [13]. Cavern pressure build-up, then, is a function of time as well as of cavern depth. According to formula (1) or (2), the effects of cavern depth are two-fold:

(i) it increases the initial difference between geostatic pressure $[P_\infty\,(\text{MPa}) = 0.022H\,(\text{m})]$ and the initial halmostatic pressure $[P_i = P_h\,(\text{MPa}) = 0.012\,H\,(\text{m})]$; and

(ii) it increases the average rock temperature, which influences rock-salt creep and results in a much faster creep rate (and subsequent pressure build-up rate) in a deeper cavern.

Both lead to a much faster initial pressure build-up rate in a deep closed cavern. A general discussion can be found in Bérest et al. [16].

2.2. Brine thermal expansion

The temperature of rock salt increases with depth, a typical value being $T_R = 45°C$ at a depth of $H = 1000\,\text{m}$, but caverns are leached using soft water pumped from shallow aquifers whose temperatures can be 15°C. The transit time of water in the cavern during leaching is generally a few days (or weeks in a larger cavern), which means that brine temperature in the cavern during (and at the end) of leaching is close to the soft water temperature (say, brine temperature is $T_0 = 20°C$ at a 1000-m depth.) When the cavern remains idle, after leaching is completed, the initial temperature difference $(T_R - T_0 = 45 - 20 = 25°C$ in the example) will slowly resorb with time, due to heat conduction through the rock to the cavern and heat convection in the cavern.

Appropriate heat-transfer equations can be written as follows:

$$\frac{\partial T}{\partial t} = k\,\Delta T, \tag{3}$$

$$\int_\Omega \rho_b C_b \dot{T}_i d\Omega = \int_{\partial\Omega} \tilde{K}\partial T/\partial n\,da, \tag{4}$$

$$T_i(t) = T_{wall}. \tag{5}$$

The first equation holds inside the rock-salt mass (k is the thermal diffusivity of salt, which has a typical value of $k = 3 \times 10^{-6}\,\text{m}^2/\text{s} \approx 10\,\text{m}^2/\text{yr.}$); the second equation is the boundary condition at cavern wall: heat flux crossing a cavern wall ($\tilde{K}$ is the thermal conductivity of salt; $\tilde{K} \approx 6\,\text{W/m/}°C$ is typical) warms up cavern brine with an average temperature of T_i ($\rho_b C_b$ is the volumetric heat capacity of brine; $\rho_b C_b \approx 1200 \cdot 4000 = 4.8 \times 10^6\,\text{J/m}^3/°C$ is typical, see *Physical Properties Data for Rock Salt* [28]). The third equation stipulates that rock temperature of the cavern wall is equal to the average brine temperature in the cavern which is assumed to be homogeneous. This assumption is reasonable due to the effect of cavern brine stirring due to thermal convection. Clear evidence of thermal convection effects can be found in Fig. 4, which provides the temperature distribution in the 950-m deep Ez53 cavern; the temperature in the cavern appears quite homogeneous, due to thermal convection patterns.

The exact temperature evolution can easily be predicted through numerical calculation. Back-of-the-envelope estimations can be reached simply by the analysis of heat transfer equations. Dimensional analysis of Eq. (3) proves that heat transfer is governed by one characteristic time, for instance, $t_c = V^{2/3}/(4k)$ [or $t_c\,(\text{years}) = V^{2/3}/400$, where V is the cavern volume (in m^3)]; the second characteristic time, deduced from
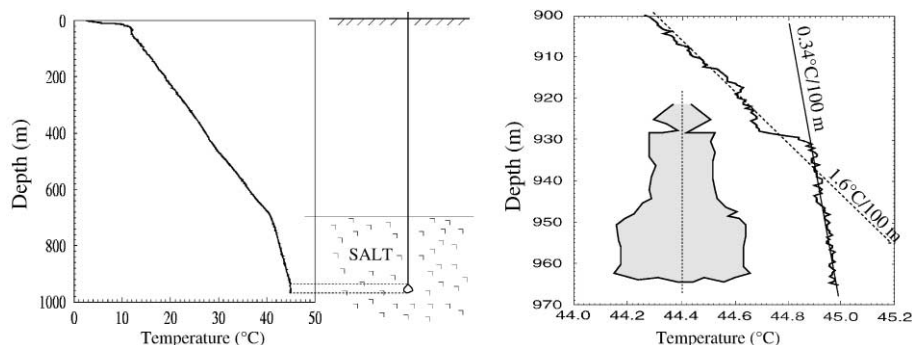

Fig. 4. Geothermal profile in the Ez53 cavern and well (February 1996). Note that brine temperature in the cavern is quite homogeneous, due to natural free convection.

Eq. (4), $t'_c = kt_c\rho_b C_b / \tilde{K}$, is not significantly different from t_c. In the case of a spherical cavern, t_c is the time after which approximately 75% of the initial temperature difference between the brine and the rock mass has been resorbed; brine heating will be slightly faster in a cylindrical cavern. This characteristic time is large ($t_c \approx 1$ year for a $V = 8000 \text{ m}^3$ cavern; $t_c \approx 16$ years for a $V = 500,000 \text{ m}^3$ cavern), which means that thermal equilibrium will be reached after a long period of time.

The average temperature change rate (from leaching completion time $t = 0$ to characteristic time $t = t_c$) is $\dot{T}_i \approx 0.75\,(T_R - T_0)/t_c$ — i.e., where $T_R - T_0 = 25°C$, $\dot{T}_i \approx 18°C/\text{yr}$ in an 8000 m^3 cavern and $\dot{T}_i \approx 1.2°C/\text{yr}$ in a $500,000\text{ m}^3$ cavern. In an opened cavern, a temperature increase leads to thermal expansion and brine outflow at ground level, $Q = \alpha V \dot{T}_i$, where α is the brine thermal expansion coefficient, $\alpha \approx 4.4 \times 10^{-4}°C^{-1}$ [29]. In a closed cavern, temperature increase leads to pressure build-up (i.e., $\dot{P}_i = \alpha \dot{T}_i / \beta$.) The ratio α/β is close to $1\,\text{MPa}/°C$, which means that a $1°C$ brine temperature increase leads to a 1-MPa pressure build-up. In other words, when an initial temperature difference of $25°C$ is resorbed, after a time equal to several times t_c, the related pressure build-up should be $25\,\text{MPa}$ — far exceeding the initial difference between geostatic and halmostatic pressure — and possibly leading to salt fracture. How fast this difference is resorbed depends on cavern size; the initial rate is typically $18\,\text{MPa/yr}$ in an 8000-m^3 cavern and $1.2\,\text{MPa/yr}$ in a $500,000\text{-m}^3$ cavern. Keep in mind that creep effect in a 1000-m deep cavern leads to a typical pressure build-up change rate of $0.75\,\text{MPa/yr}$ (Section 2.2); it is clear that, in most cases, pressure build-up due to thermal expansion predominantly governs the behavior of a closed cavern. Outstanding exceptions are found in the case of very deep caverns (2000 m below ground level; see You et al. [2]), creep-prone evaporitic layers (see Fokker [4]) or brine fields whose extraction ratios are high [30]. This thermal expansion effects must be avoided when closing a cavern, as temperature increase and resulting pressure build-up lead to cavern fracturing. However, and clearly different from cavern creep effects in this respect, brine expansion effects can be avoided — for instance, by waiting a sufficient amount of time before closing the cavern (i.e., until thermal equilibrium is reached).

2.3. Fracture risk

If brine thermal expansion (which leads to fracture) is disregarded, one can expect that cavern creep will end when brine pressure in the cavern exactly equals overburden (i.e., geostatic) pressure at cavern depth; however, such an equilibrium does not exist, as has been clearly demonstrated by Wallner [9], Cauberg et al. [10], and Wallner and Paar [13], Ehgartner and Linn [15]. As stated above, rock salt behaves as a liquid when long periods of time are considered: two liquids whose densities are distinct, as is clearly the case when brine and rock salt are considered, cannot reach equilibrium unless they are separated by a flat, horizontal interface. In simpler words, brine pressure in the cavern cannot equal rock pressure at both the top and bottom of the cavern. In the final state, brine pressure at the cavern top will exceed the geostatic pressure by an amount which depends on cavern height. Then an extensive (or tensile) state of stress prevails at cavern wall: the two (negative) tangential stresses are equal and larger than the (negative) radial stress, $\sigma_{\theta\theta} = \sigma_{\varphi\varphi} > \sigma_{rr} = -P_i$ and the effective tangential stress $\sigma_{\theta\theta} + P_i$ is a tensile stress. In this context, salt behavior is fragile; the tensile strength of the rock will probably be exceeded at the top of the cavern, and fracture risk will become highly probable. Furthermore, fracture is likely to develop upward (except perhaps in a strongly interbedded salt layer), increasing the total (cavern + fracture) height and leading to further upward movement of the fracture and brine transport through the fracture.

2.4. Effect of permeability

This pessimistic scenario can be alleviated by taking rock-salt permeability into account. For every standard engineering purpose, rock salt can be considered as an impermeable rock. The generally small permeability numbers resulting from laboratory tests are scattered, but they are suspect of being influenced by several biases (sampling, rock decompression, etc.). Few in situ tests are available; experiments performed at the WIPP site [31] provide permeabilities as small as $K = 10^{-21} \text{ m}^2$ for undisturbed salt. A 1-year-long test, performed in a well and supported by the SMRI [32], gave $K \approx 6 \times 10^{-20} \text{ m}^2$. How small these numbers are is clearly demonstrated when one remembers that hydrogeology textbooks generally define an impermeable rock as a one whose permeability is smaller than $K = 10^{-17} \text{ m}^2$, a figure that exceeds the measured values described above by two orders of magnitude or more. It means that, when short term use of salt caverns is considered, for instance when hydrocarbons are stored, salt caverns can be considered to be extremely safe from the perspective of product confinement.

However, when very long-term behavior is considered, the general picture changes — especially when considering the problem of pressure build-up in a closed cavern. Due to high cavern compressibility, even tiny losses of fluid can significantly lessen the effect of cavern creep and prevent cavern pressure from reaching high levels.

To be more specific, consider the case of a spherical cavern with radius R, excavated in a salt mass with permeability K, cavern brine pressure P_i and natural

pore brine pressure P_o. If η is the brine dynamic viscosity ($\eta \approx 1.2 \times 10^{-3}$ Pa.s [16]) then, assuming Darcy's law — a somewhat arguable hypothesis — steady-state brine seepage rate will be of the order of

$$Q_b/V = 3K(P_i - P_o)/(\eta R^2). \qquad (6)$$

This rate is quite small (for instance, $P_i - P_o = 5$ MPa, $R = 12.5$ m ($V = 8000$ m^3), and $K = 10^{-20}$ m^2 leads to $Q_b/V \approx 0.25 \times 10^{-4}$ yr^{-1}, or 0.2 m^{3}yr^{-1}), but it can balance creep rate, especially when cavern brine pressure is high. One example (for the Ez53 cavern) will be discussed later.

It must be outlined that the concept of a homogeneous isotropic permeability (i.e., a uniform value of K through the whole salt mass) is probably incorrect. The Durup's test mentioned above [32] proved that a linear relation did exist between brine seepage and pressure build up in an Etrez well. But the Etrez upper salt layer, which is concerned by the described test, is known to contain a 10% volume of impurities, anhydrite layers (such as is visible at a 928-m depth on Ez53 cavern profile, see Fig. 4) and thin intergranular clay layers, whose permeability can be suspected of being much larger than the permeability of rock salt, leading to higher large-scale permeability of the formation. On the other hand, since the end of the leaching period (1982) to the described test period (1997), the Ez53 cavern has experienced significant cumulated deformations, within the range $10^{-3} - 10^{-2}$. They may have led to cavern wall damage, especially along the interface between salt and stiffer anhydrite layers, inducing localized permeability changes. In other words, formula (6) appears as a rule of thumb rather than the exact mathematical consequence of a well-stated phenomenon, and the introduction of coefficient K must be considered as a tentative definition of an "equivalent" or "average" permeability.

3. Test preparation

The objective of the test described in this paper was to verify that pressure build-up in a closed and abandoned cavern does not reach geostatic values but, rather, due to the combined effects of salt creep and salt (micro) permeability, will vanish when a certain steady-state value of the cavern pressure (significantly smaller than the geostatic figure) is reached.

3.1. Main goals and prerequisites

Because we are interested in the combined effects of creep and percolation, test conditions must be selected to minimize the effect of the third factor contributing to pressure changes, i.e., thermal expansion. Keep in mind that the expression of the characteristic time of thermal conduction is $t_c = V^{2/3}/(4k)$; thus, it is necessary to use a cavern that is small and/or has been leached out long before the test. The Ez53 cavern of the Gaz de France storage site in Etrez (Fig. 4), in South-eastern France, meets these conditions: it was leached out in Spring 1982 (i.e., 15 years before the test), and its volume is small ($V \approx 7500$ m^3), which means that the characteristic time of thermal conduction in this cavern is approximately $t_c = 1$ year.

The thermal behavior of Ez53 during the first year after the end of leaching was monitored via cavern brine-temperature measurements [14] that confirmed that approximately 65% of the initial temperature difference between the rock mass and the cavern brine had already been resorbed after 250 days (in February 83). Temperature profiles were performed in February (Fig. 4) and March 1996 and clearly prove that thermal equilibrium was reached at that time. From then on, cavern behavior is governed only by cavern creep and brine permeation.

The average cavern depth is 950 m; at such depth, moderate creep rates are expected. Brine outflow from the opened cavern (brine permeation is then null) was measured for several weeks before the test; these measurements are described in Brouard [33] and prove that the cavern convergence rate is approximately 3×10^{-4} yr^{-1}. Because the cavern had been at rest for most of the time since the end of leaching, this figure is considered to be representative of steady-state cavern creep. It must be noted that the Etrez site cavern closest to Ez53 is Ez04, which is 1 km away, precluding any significant mechanical influence of neighboring caverns.

The rock salt belonging to the so-called upper layer of the Etrez salt formation, in which the cavern has been leached, has been studied by Charpentier [34] and Pouya [35]. The latter has fit laboratory data to the Norton–Hoff uniaxial constitutive (or power) law described above and suggests the following parametric values:

$$A = 0.64 \text{ MPa}^{-n} \text{ yr}^{-1}, \quad \mathcal{Q}/\mathcal{R} = 4100 \text{ K}, \quad n = 3.1,$$

which are in good agreement with the in situ observations. In fact, a simple estimation can be reached by considering the case of a spherical cavern located at the Ez53 cavern depth (see formula 1); the above-cited values then lead to a steady-state cavern creep rate of 3×10^{-4} yr^{-1}. Such perfect agreement between the observed and computed figures must be considered as partly fortuitous, but it does provide some confidence in the estimation.

Note that the steady-state law is not able, as stated above, to capture the effects of rapid changes in cavern pressure. The so-called Lemaitre strain-hardening constitutive law, based on in situ pressure tests carried out by Gaz de France [14], appears to provide satisfactory predictions.

Etrez salt permeability has been studied through laboratory experiments by Le Guen [36] who found an intrinsic permeability as low as $K = 10^{-21}$ m^2 for some samples. According to the generally accepted effects of scale on rock permeability [37], larger values are expected when in situ measurements are considered. In fact, Durup [32] has performed an in situ permeability test, discussed above on the Ez58 well, which belongs to the same salt formation as the Ez53 cavern and has similar depth. Durup found that pore pressure, P_o, was very close to halmostatic pressure ($P_h \approx P_o$) and suggested a value of $K = 6 \times 10^{-20}$ m^2 for the average intrinsic permeability of the 150-m high Ez58 well.

Assuming both steady-state cavern creep and steady-state brine percolation (as well as Darcy's law), the long-term equilibrium pressure can be computed by making the cavern creep rate and the relative brine leak rate equal (see [16]):

$$\frac{3K}{\eta R^2}(P_i - P_o) = A^* \exp\left(-\mathscr{Q}/\mathscr{R}T\right)(P_\infty - P_i)^n, \qquad (7)$$

$$A^* = \frac{3}{2}\left[\frac{3}{2n}\right]^n A,$$

$K = 6 \times 10^{-20}$ m^2, $R = 12.1$ m, $P_o = 11.2$ MPa,

$\eta = 1.2 \times 10^{-3}$ Pa.s, $\mathscr{Q}/\mathscr{R} = 4100$ K, $T = 318$ K

$A^* = 0.14$ MPa^{-n}yr^{-1}, $P_\infty = 20.5$ MPa, $n = 3.1$.

when Ez58 (permeability) and Ez53 (creep) parameters are used. In the case of a spherical cavern, we get $P_i \approx 14.3$ MPa; the brine leakage through the cavern wall is then 0.8 m^3/yr^{-1}. As we will see, the actual pressure value appears to be smaller. Returning to the general formula (7), it is clear that, the larger (R large) or deeper (T, P_o, and P_∞ large) the cavern, the higher the equilibrium pressure.

4. Operation

4.1. Testing program

The test basically consists of a "trial and error" process (Fig. 5) to approach the expected steady-state pressure, which was roughly estimated before the test (see the last section.) Different pressure levels are tested successively. When the well-head pressure rate consistently remains negative for a sufficiently long period of time, it is re-adjusted to a slightly smaller value, in hopes of triggering a change in sign for the well-head pressure rate. Alternatively, when the well-head pressure rate consistently remains positive for a sufficiently long period of time, it is re-adjusted to a slightly higher value. Re-adjustments are made via small withdrawals or injections of brine and/or fuel-oil in the cavern.
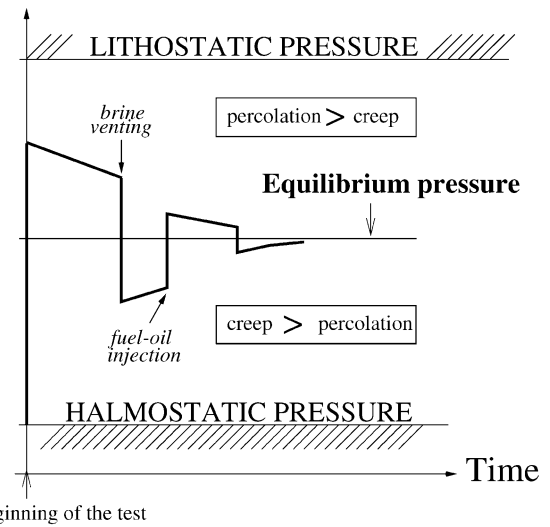

Fig. 5. Test strategy: "trial and error". The exact equilibrium pressure, which is unknown at the beginning of the test, is found out through a trial and error procedure.
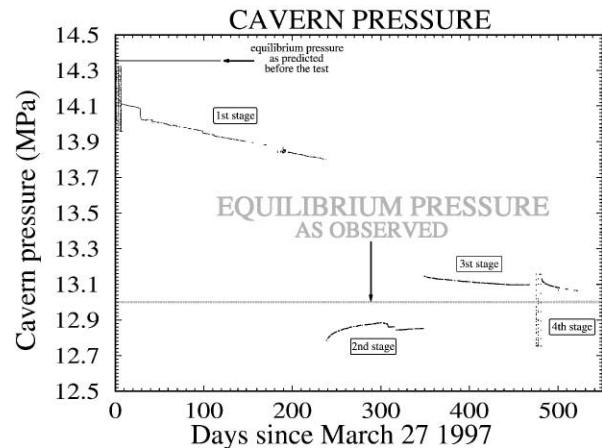

Fig. 6. Cavern pressure evolution during the test.

The timing of each step between injection and withdrawal (or vice versa) must be thoroughly examined. It is well known that any rapid pressure change (such as takes place when fluid injection or withdrawal is performed) triggers transient effects (e.g., transient creep, additional dissolution or crystallization), which, according to the general Le Chatelier (or Braun) principle, tend to reduce the pressure change slightly (see above). Thus, each step must be long enough for these transient effects to vanish and for a more-or-less steady state to be reached. Former tests [14] have proven that in this cavern transient effects following any rapid pressure change were most significant during a period of approximately 12 days. During the test described below (see Fig. 6), the duration of each step was long enough (longer than 3 months) to allow transient effects to vanish.

Redundant pressure measurements were necessary to provide reliable results. Cavern pressure was measured at a depth of 925 m, and pressures at the well head were measured both in the annular space (P_a) and in the central tubing (P_t). Two pressure-measurement systems were used, of which the higher resolution (± 1 kPa) system proved to be more reliable. Fig. 6 has been drawn using the data provided by this system.

The test consists of three main stages; the cavern pressure was (roughly) constant during each stage. After the test ended (day 446), a part of the measurement system was still working, and we took advantage of that to measure the pressure evolution (fourth stage) (see Fig. 6).

4.2. Casing leakage versus cavern leakage

An important difference between a shut-in test and actual cavern abandonment lay in the fact that, during a shut-in test, the cavern is closed *at the well-head* — not at the bottom of the well. As a result, brine (or, more generally, liquid) leaks can occur both in the cavern and in the well itself through the casing (or casing-shoe) or through the well-head. Such leaks are known to have occurred in some underground storage environments; this is why casings are thoroughly checked prior to commissioning, and intermittently during the cavern life span, through tests generally referred as "Mechanical Integrity Tests" or MIT, Crotogino [38]. A typically recommended resolution of such a test is 50 m³/yr, much larger than the absolute values considered during the described test. The existence of such leaks would lead to severe misinterpretation of the test if casing leakage and brine percolation through the cavern wall were not distinguished.

We have designed a system based on the density difference between brine and fuel-oil that allows differentiation of cavern brine seepage (the topic of interest) and well leakage. The system is similar to that suggested by Diamond et al. [39] for testing brine production wells.

Well completion includes a 24.45 cm ($9^{5/8''}$) cemented casing and a 17.78 cm ($7''$) string. Before the test on March 20, 1997 (day -7), a fuel-oil column was lowered to a depth of 864.5 m in the 17.78 cm × 24.45 cm ($7'' \times 9^{5/8''}$) annular space, where the horizontal cross-section is approximately $\Sigma = 5.7$ l/m.

On November 20 (day 238), the system was completed by lowering a smaller fuel-oil column into the 17.78 cm ($7''$) central tubing, to an approximate depth of 9.5 m. (It would have been better to set this second column before the test.) The horizontal cross-section of the tubing is constant and approximately equal to $S = 21.1$ l/m. The monitoring system was then completed; however, following the leaks in days 293–315, additional fuel oil was injected (on March 10, 1998; day 348) into the 17.78 cm ($7''$) central tubing, which lowered the fuel-oil/brine interface to an approximate depth of 43 m.

This system allows easy comparison of the various types of leaks (see Fig. 7). Let $\dot{V}$ be the cavern volume loss rate due to creep, $\dot{V} < 0$; Q_b is the brine outflow from the cavern to the rock mass through the cavern walls; Q_a is the fuel-oil leakage rate through the casing (or casing shoe); Q_t is the fuel-oil leakage rate through the well head. A brine leak (Q_b) from the cavern generates the same pressure drop rate ($\dot{P}_i$) in the cavern as well as in both the annular space ($\dot{P}_a$) and the central tubing ($\dot{P}_t$) at the well head: $\dot{P}_i = \dot{P}_a = \dot{P}_t = -Q_b/(\beta V)$, where βV is the cavern compressibility, as defined above. Brouard [33] has measured compressibility of the Ez53 cavern as approximately $\beta V \approx 3$ m³/MPa, in other words, brine seepage of 3 l/day will lead to a pressure drop rate of 1 kPa/day.

An example of this is given in Fig. 8. During days 112–146, the average pressure drop rate is -869.70 Pa/day in the annular space and -869.85 Pa/day in the central tubing; the two curves (pressure versus time) are then almost perfectly parallel, proving that seepage takes place in the cavern itself (in sharp contrast to what happens in the case of a fuel-oil leak.) During this period, brine seepage from the cavern (or, more precisely, the difference ($Q_b - |\dot{V}|$) between brine seepage and cavern creep) is $3 \times 0.87 = 2.6$ l/day. Note that very small oscillations (period ≈ 12 h, amplitude ≈ 0.5 kPa) can sometimes be observed on the two curves; these are related to terrestrial tidal waves and ground-level temperature changes.

A fuel-oil leak (Q_t) from the central tubing through the well head will produce a similar pressure drop both in the cavern and in the annular space — i.e., $\dot{P}_i = \dot{P}_a = -Q_t/(\beta V)$. However, brine density ($\rho_b = 1200$ kg/m³) is significantly larger than fuel-oil density ($\rho_f = 850$ kg/m³); a fuel-oil leak yields to both an upward vertical displacement of the brine/fuel-oil interface and an additional pressure drop in the central tubing, $\dot{P}_t = \dot{P}_a - (\rho_b - \rho_f)gQ_t/S$, where $S = 21.1$ l/m is the 17.78 cm ($7''$) central tubing cross-section. A fuel-oil leak from the annular space acts in the reverse: the pressure drop rate in the tubing is simply $\dot{P}_t = \dot{P}_i = -Q_a/(\beta V)$ and is $\dot{P}_a = \dot{P}_t - (\rho_b - \rho_f)gQ_a/\Sigma$ in the annular space, whose cross-section is $\Sigma = 5.7$ l/m. As a whole, when taking into account the cavern-volume loss rate, we get the following formulae:

$$\left.\begin{array}{l} \dot{P}_a \\ \dot{P}_t \end{array}\right\} = -\frac{Q_b + Q_a + Q_t - |\dot{V}|}{\beta V} - (\rho_b - \rho_f)g \left\{ \begin{array}{l} Q_a/\Sigma, \\ Q_t/S. \end{array} \right.$$

(8)

Fig. 9 provides an example of the pressure difference between the annular space and the central tubing, as measured through the 1 kPa resolution pressure gauges
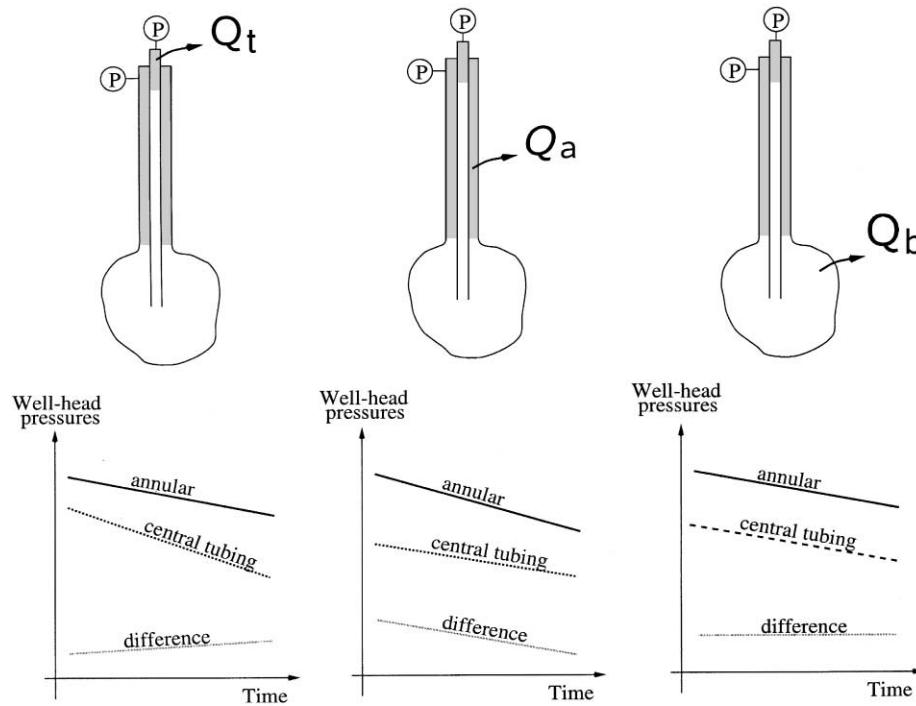
Fig. 7. Three kinds of possible leaks; they can be discriminated through observation of well-head pressures evolution.
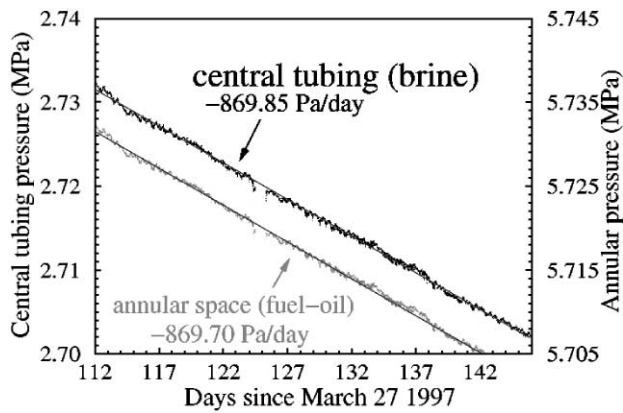

Fig. 8. Annular and tubing pressure variations from days 112 to 150. Difference is almost null, precluding any significant leakage through central tubing or cemented casing.
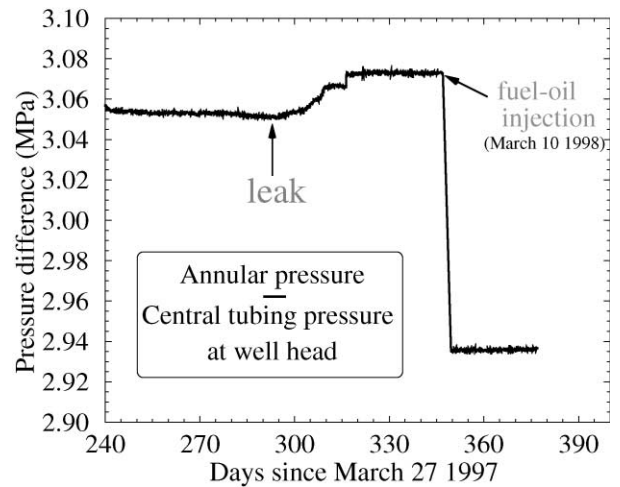

Fig. 9. Pressure difference between annular and tubing from days 240 to 375. (The increasing pressure difference indicates leakage from the tubing. A pressure increase of 0.01 MPa is equivalent to a 60-l leak. The decreasing pressure difference indicates leakage from the annular space. A pressure decrease of 0.01 MPa is equivalent to a 16-l leak.)

(see below) and plotted versus time. Between days 240 and 293 the difference is fairly constant — as a matter of fact, there is a slight negative slope, approximately 60 Pa/day. On day 293, a rapid and severe increase of the pressure difference takes place — clear evidence of a fuel-oil leak through the central tubing well head. The cumulated differential pressure increase is $\delta P_a \approx 21$ kPa, which proves that the fuel-oil leak during this phase is $V_a = S\delta P_a/g(\rho_b - \rho_f) = 21/0.17 \approx 124$ l; the interface has risen by 6 m in the central tubing. On day 315, the leak was repaired. (Note that the leak had been detected

through curve observation before being observed in the field.); afterwards the pressure difference remained constant.

In conclusion, field data allow for a clear distinction between brine seepage (from the cavern) and fuel-oil leakage (from the well), precluding any misinterpretation.

5. Test results

5.1. Main results

- One month before the test (i.e., before March 27, 1997), a tubing pressure of approximately 3.1 MPa (resulting in a cavern pressure of $P_i = 3.1 + 11.2 = 14.3$ MPa) was applied in order to avoid a too steep pressure change at the beginning of the test (such a steep pressure change is known to trigger transient creep).
- From day 1 (March 27, 1997) to day 238 (November 19, 1997), the well-head pressure decreased by a roughly constant rate of $\dot{P}_i = -0.9$ kPa/day, or an apparent leak of $Q_b - |\dot{V}| = 2.7$ l/day, with the initial well-head pressure being $P_a = 2.92$ MPa (14.13 MPa at a depth of 950 m). During this stage, permeation effects clearly prevail over creep effects: Brouard [33] measured a 7 l/day brine flow due to cavern creep when cavern pressure was 11.2 MPa; then according to the $n = 3.1$ exponent proposed by Pouya [35] for the steady-state creep law, cavern creep should be $\dot{V} = -2.5$ l/day when cavern pressure is 14.13 MPa — which means that the total brine leak through cavern walls during this stage is $Q_b = 2.7 + 2.5 = 5.2$ l/day.
- On day 238, cavern pressure was lowered by 1 MPa, and some fuel oil was injected in the central tubing (to complete the monitoring system described above). Up to day 250, the average pressure build-up rate was 6.1 kPa/day (the influence of transient creep was probably very significant during this 12-day period), and then slowly decreased. Its average value was $\dot{P}_i = +0.6$ kPa/day between days 275 and 290: creep prevailed over permeation. A fuel-oil leak appeared around January 25, 1998: as described above, it was first detected when analyzing pressure measurements and then observed in situ and repaired. Between days 320 and 345, the average pressure build-up rate was $\dot{P}_i = 0.32$ kPa/day.
- On day 348, a small amount of fuel oil was injected in the central tubing, leading to a 0.3 MPa increase of cavern pressure. From then until day 446, cavern pressure decreased by $\dot{P}_i = -0.44$ kPa/day on average.
- From day 446 to 540, several fluid injection or withdrawals occurred. During a 20-day period, the cavern pressure, which was then smaller than 12.5 MPa, built-up; later, over a longer period, the cavern pressure, which was 13.1 MPa, slowly decreased.

From these results, it can be inferred that the equilibrium cavern pressure decreases when higher than $P_i = 13.0 \pm 0.1$ MPa (permeation prevails over creep) and increases when smaller than this value (creep prevails over permeation). The "equilibrium pressure" is much smaller than the geostatic pressure, which is $P_\infty = 20.5$ MPa, and slightly smaller than expected before the test ($P_i = 13.0 \pm 0.1$ MPa instead of 14.3 MPa). This discrepancy may be due to an initial underestimation of the permeability of a full-sized cavern.

While Ez53 creep, which had been measured through in situ tests, can be considered to have been reasonably well estimated, it is logical to conclude that cavern permeability, which can be back-calculated using (6), must be larger than the value estimated earlier [32] through well tests and can be $K = 2 \times 10^{-19}$ m^2; the variations of cavern volume and brine volume are then of the order of $Q_b = |\dot{V}| = 1.4$ m^3/yr — or 5 kg/day, or 2×10^{-4} yr^{-1} when compared to overall cavern volume.

5.2. Long-term evolution of a sealed cavern

The test results show that cavern sealing in the Etrez site will not lead to fracture of the salt mass — provided that thermal expansion can be disregarded — and brine pressure will not exceed a figure smaller than a geostatic value. This should be true even when the cavern has experienced large losses of volume; formula (7) proves that the equilibrium pressure is a decreasing function of cavern size because the surface/volume ratio is larger in a small cavern, making brine permeation more effective. After a long period of time, a large volume of rock salt around the cavern will be impregnated by brine expelled from the cavern. A full description of this process is still under investigation.

Finally, it must be noted that the Etrez salt formation, which contains a significant amount of impurities, appears to be relatively permeable. Several authors argue that other salt formations are far more impermeable. (For instance, Klafki et al. [40] recommend $K < 10^{-20}$ m^2 as a general rule.) However, such theories are often based on small-scale permeability tests, whose relevance for the problem of large cavern tightness is arguable; large scale permeability of salt formations remains an opened question.

5.3. Practical recommendations for cavern abandonment

From a practical point of view, the following steps can be recommended when planning cavern abandonment:

1. The thermal expansion of brine leads to a large pressure build-up that can lead to fracture, brine migration and subsidence, which must be avoided to prevent the overlying water-bearing strata pollution. Before sealing a cavern, the brine temperature must be measured and compared to the natural rock temperature at cavern depth. A 1°C, difference can lead to a 1-MPa pressure build-up after sealing. If thermal equilibrium is not reached by the time the

cavern is to be sealed, two remedial actions can be considered:

(i) wait for thermal equilibrium to be reached, which sometimes takes a long time; or
(ii) inject a small amount of inert gas into the cavern to increase its compressibility.

2. When thermal expansion can be disregarded, an equilibrium pressure will be reached when cavern creep and brine seepage are exactly equal. Cavern creep can be estimated through laboratory experiments and numerical computations, or through brine outflow tests (the daily brine flow from the cavern is measured for a few days; correct interpretation is much easier when thermal equilibrium has already been reached). Brine seepage is preferably estimated through in situ permeability tests performed in a well before leaching. Simple calculations then allow estimation of the equilibrium pressure.

3. Before sealing the cavern, additional brine can be injected in the cavern to reach a pressure slightly higher than the anticipated equilibrium pressure (checking that pressure rate remains negative after 1 month). During such a test, the absence of a leak from the well must be checked thoroughly to prevent misinterpretation. An accurate method based on the injection of fuel oil in the well has been suggested in this paper.

6. Conclusions

The 18-month long test (a "shut-in pressure test") performed on the Ez53 cavern proves that brine pressure reaches an equilibrium value of $P_i = 13. \pm 0.1$ MPa at a depth of 950 m, which is significantly smaller than the geostatic pressure ($P_\infty = 20.5$ MPa) at the considered depth. This equilibrium is reached when cavern creep (which leads to cavern shrinkage) exactly equals brine permeation toward the rock mass (which reduces the brine volume contained in the cavern).

Brine permeation flow rate is quite small ($1.4\,\mathrm{m^3/yr}$); at such a rate, the initial brine bubble contained in the cavern will vanish into the salt formation after 50 centuries. This test confirms that salt formation permeability must be taken into account when analyzing cavern abandonment conditions: salt permeability can prevent large pressure build-up in an abandoned cavern, then avoiding fracture creation and rapid fluid seepage to shallow water-bearing formations, a pessimistic scenario considered by many authors. Test results suggest that pressure build-up will remain moderate, and final equilibrium pressure will be significantly lower than geostatic pressure.

Further works are still needed. These conclusions are relative to a salt formation which contains impurities. The concept of an "equivalent" homogeneous permeability of the salt formation is open to critics, and will require further investigations. Evolution of the permeability with time, including microfracturation and healing, are to be thoroughly discussed. The performed test proves that long-term cavern evolution involves a complex combination of physical processes; recent significant advances give some confidence in a better understanding of their effects.

References

[1] Bérest P, Ledoux E, Legait B, de Marsily G. Effets thermiques dans les cavités en couches salifère. Proceedings of Fourth ISRM Congress, vol. I. Rotterdam: Balkema, 1979. p. 31–5.
[2] You T, Maisons C, Valette M. Experimental procedure for the closure of the brine production caverns on the "Saline de Vauvert" site. Proceedings of SMRI Fall Meeting, Hannover, 1994 (Proceedings of the "SMRI Meetings" are available at: SMRI-3336 Lone Hill Ln., Encinitas, CA 92024-7262, USA).
[3] Van Sambeek LL. A simple method for modeling the pressure build up or flow of an abandoned solution well. Proceedings of SMRI Spring Meeting, Austin, 1990.
[4] Fokker PA. The behavior of salt and salt caverns. PhD thesis, Delft University of Technology, The Netherlands, 1995.
[5] Bérest P, Brouard B, Durup G. Abandon des cavités salines. Rev Fr Géotech 1998;(82):23–36.
[6] Bérest P, Brouard B, Durup G. Shut-in pressure tests — Case studies. Proceedings of SMRI Fall Meeting, San Antonio, 2000. p. 105–26.
[7] Tomasko D, Elcock D, Veil J, Caudle D. Risk analyses for disposing of nonhazardous oil field wastes in salt caverns. Argonne National Laboratory, US Department of Energy, Contract W-31-109-ENG-38, 1997.
[8] Langer M, Wallner M, Wassman W. Gebirgsmechanische Bearbeitung von Stabilitäts fragen bei Deponiekavernen im Salzgebirge, Kali und Steinsaltz, vol. II. Germany: Verlag Glückhauf, 1984. p. 66–76.
[9] Wallner M. Frac-pressure risk in rock salt. Proceedings of SMRI Fall Meeting, Amsterdam, 1986.
[10] Cauberg H, Kuilman B, Valkering B, Walters JV. Rock mechanical behavior and sealing aspects of a closed-in salt cavity filled with brine. SMRI Fall Meeting, Amsterdam, 1986.
[11] Bérest P. Les problèmes soulevés par l'abandon des cavités de dissolution profondes dans le sel gemme. In: Stockage en souterrain. Presses des Ponts et Chaussées, Paris, 1990. p. 115–30.

[12] Rolfs O, Schmidt U, Crotogino F. Rock mechanical studies on the post-operational phase of a disposal cavern. Proceedings of Third Conference on Mechanical Behaviour of Salt. Clausthal-Zellerfeld, Germany: Trans Tech Pub, 1996. p. 417–26.

[13] Wallner M, Paar WA. Risk of progressive pressure build up in a sealed cavity. Proceedings of SMRI Fall Meeting, El Paso, 1997. p. 177–88.

[14] Hugout B. Mechanical behavior of salt cavities — in situ tests — model for calculating the cavity volume evolution. Proceedings of Second Conference on Mechanical Behaviour of Salt. Clausthal-Zellerfeld, Germany: Trans Tech Pub., 1988. p. 291–310.

[15] Ehgartner BL, Linn JK. Mechanical behavior of sealed SPR caverns. Proceedings of SMRI Fall Meeting, Houston, 1994.

[16] Bérest P, Brouard B, Durup G. Behavior of sealed solution-mined caverns. Proceedings of Fourth Conference on Mechanical Behaviour of Salt. Clausthal-Zellerfeld, Germany: Trans Tech Pub., 1997. p. 511–24.

[17] Ghoreychi M, Cosenza P. Quelques aspects de la sûreté à long terme de stockages dans le sel. Proceedings of 4ème Colloque franco-polonais, ISBN 2-85555-048-3, 1993. p. 209–18.

[18] Cosenza P, Ghoreychi M. Coupling between mechanical behavior and transfer phenomena in salt. Proceedings of Third Conference on Mechanical Behaviour of Salt. Clausthal-Zellerfeld, Germany: Trans Tech Pub., 1996. p. 285–307.

[19] Pfeifle TW, DeVries KL, Nieland JD. Damage-induced permeability enhancement of natural rock salt with implications for cavern storage. Proceedings of SMRI Spring Meeting, New Orleans, 1998. p. 260–89.

[20] Hardy RH, Langer M. Proceedings of First Conference on Mechanical Behaviour of Salt. Clausthal-Zellerfeld, Germany: Trans Tech Pub., 1984. p. 901.

[21] Hardy RH, Langer M. Proceedings of Second Conference on Mechanical Behaviour of Salt. Clausthal-Zellerfeld, Germany: Trans Tech Pub., 1988. p. 781.

[22] Hardy RH, Langer M, Bérest P, Ghoreychi M. Proceedings of Third Conference on Mechanical Behaviour of Salt. Clausthal-Zellerfeld, Germany: Trans Tech Pub., 1996. p. 621.

[23] Aubertin M, Hardy RH. Proceedings of Fourth Conference on Mechanical Behaviour of Salt. Clausthal-Zellerfeld, Germany: Trans Tech Pub., 1997. p. 658.

[24] Van Sambeek LL. Evaluating cavern tests and surface subsidence using simple numerical model. Proceedings of Seventh Symposium on Salt, vol. I. Amsterdam: Elsevier Science Publishers B.V., 1992. p. 433–9.

[25] Brouard B, Bérest P. A tentative classification of salts according to their creep properties. Proceedings of SMRI Spring Meeting, New Orleans, 1998. p. 18–38.

[26] Bérest P, Bergues J, Brouard B. Review of static and dynamic compressibility issues relating to deep underground salt caverns. Int J Rock Mech Min Geol. Abstr 1999;36:1031–49.

[27] Bérest P, Bergues J, Brouard B. Anharmonic oscillations in underground cavities. CR Acad Sci Paris, série II b, 1997;325:701–7.

[28] US Department of Commerce. In: Gevantman LH, editor. Physical properties data for rock salt. National Bureau of Standards (U.S.), Mono. 167. 1981. p. 288.

[29] Boucly P. Expériences in situ et modélisation du comportement des cavités utilisées pour le stockage du gaz. Rev Fr Géotech 1982;(18):49–58.

[30] Guarascio M, Fernandez G. In situ testing for rock salt characterization. Proceedings of SMRI Fall Meeting, Roma, 1998. p. 179–219.

[31] Howarth SM, Peterson E, Lagus PL, Lie KH, Finley SJ, Nowak EJ. Interpretation of in situ pressure and flow measurements of the Salado formation at the Waste Isolation Pilot Plant. SPE Paper 21840, 1991.

[32] Durup JG. Long term tests for tightness evaluations with brine and gas in salt. Proceedings of SMRI Fall Meeting, Hannover, 1994.

[33] Brouard B. Sur le comportement des cavités salines, Etude théorique et expérimentation in situ. PhD thesis, Ecole polytechnique, France, 1998.

[34] Charpentier JP. Creep of rock salt at elevated temperature. Proceedings of Second Conference on Mechanical Behaviour of Salt. Clausthal-Zellerfeld, Germany: Trans Tech Pub., 1988. p. 131–6.

[35] Pouya A. Correlation between mechanical behavior and petrological properties of rock salt. In: Roegiers JC, editor. Proceedings of 32nd US Symposium on Rock Mechanics, Rotterdam: Balkema, 1991. p. 385–92.

[36] Le Guen C. Mesure de la perméabilité de roches très peu perméables et étude de son évolution sous sollicitations thermo-mécaniques. PhD thesis, Ecole Nationale des Ponts et Chaussées, France.

[37] Brace WF. Permeability of crystalline and argillaceous rocks. Int J Rock Mech Min Sci 1980; XVII: 241–51.

[38] Crotogino FR. External well mechanical integrity testing/performance, data evaluation and assessment. Report no. 95-0001-S for the Solution Mining Research Institute, 1994.

[39] Diamond HW, Bertram BM, French PS, Petrick GD, Schumacher MJ, Smith JB. Detecting very small casing leaks using the water-brine interface method. Proceedings of Seventh Symposium on Salt, vol. I. Amsterdam: Elsevier Science Publishers B.V., 1993. p. 363–8.

[40] Klafki M, Bannach A, Wagler T. Parameter determination for planning and constructing of gas cavern storage. Proceedings of SMRI Fall Meeting, Roma, 1998. p. 269–89.